J. Biochem. 2009;145(2)151–160
doi:10.1093/jb/mvn150

Analysis on Substrate Specificity of *Escherichia coli* Ribonuclease P Using Shape Variants of pre-tRNA: Proposal of Subsites Model for Substrate Shape Recognition

Satoshi Suwa, Yasuhiro Nagai, Akihiro Fujimoto, Yo Kikuchi and Terumichi Tanaka*
Division of Bioscience and Biotechnology, Department of Ecological Engineering, Toyohashi University of Technology, Toyohashi, Aichi 441-8580, Japan

Received October 2, 2008; accepted October 29, 2008; published online November 13, 2008

We prepared a series of shape variants of a pre-tRNA and examined substrate shape recognition by bacterial RNase P ribozyme and holoenzyme. Cleavage site analysis revealed two new subsites for accepting the T-arm and the bottom half of pre-tRNA in the substrate-binding site of the enzyme. These two subsites take part in cleavage site selection of substrate by the enzyme: the cleavage site is not always selected according to the relative position of the 3′-CCA sequence of the substrate. Kinetic studies indicated that the substrate shape is recognized mainly in the transition state of the reaction, and neither the shape nor position of either the T-arm or the bottom half of the substrate affected the Michaelis complex formation. These results strongly suggest that the 5′ and 3′ termini of a substrate are trapped by the enzyme first, then the position and the shape of the T-arm and the bottom half are examined by the cognate subsites. From these facts, we propose a new substrate recognition model that can explain many experimental facts that have been seen as enigmatic.

Key words: C5 protein, M1 RNA, ribozyme, RNase P, subsite.

Abbreviations: RNase P, ribonuclease P; pre-tRNA, tRNA precursor.

Since the discovery of catalytic RNA, many researchers have devoted themselves to studies of RNA enzymes, or ribozymes. Ribonuclease P (RNase P) is a natural ribonucleoprotein enzyme, containing an RNA subunit and a protein subunit. It processes the 5′-leader sequence of a pre-tRNA molecule to produce a tRNA (*1*). Yet researchers have struggled to reveal how the ribozyme recognizes and cleaves the pre-tRNA substrate.

Bacterial enzymes derived from *Escherichia coli* and *Bacillus subtilis* are the usual focus of study. Early studies reported the computer-modelled structure of the RNA subunit, the essential catalytic magnesium-ion-binding site, the major substrate accepting site that accepts the common CCA-3′ tag sequence of pre-tRNAs, and certain roles of the protein subunit.

Computer-modelled secondary and tertiary structures of the RNA subunit (*2–4*) have been confirmed experimentally by mutational analyses, modification analyses, cross-linking studies, and NMR and X-ray partial structural studies (*5–7*). These studies revealed a large cleft on the surface of the RNA subunit which seems to contact the top-half of a pre-tRNA molecule, and is thought to play an important role in accepting the substrate. The results also showed that the RNA subunit comprises many local small domains, most of which are conserved across species.

An essential Mg^{2+}-binding site occurs on and around the P4 and J3/4 domains (*8–11*). The conformation of these domains is important for efficient catalysis; the neighbouring P2 and P3 domains take part in stabilizing the conformation of the catalytic centre (*12–15*). Additional metal-binding sites are found on the same domains, but their role is still unclear.

In the first substrate recognition model, Kirsebom and Svard (*16*) showed that the L15/16 domain of *E. coli* ribozyme provides the accepter for the 3′-CCA tag sequence of a pre-tRNA substrate, and that the 3′-CCA sequence plays a dominant role in cleavage site selection (*17*). They also showed that the interaction between the 3′-end region of a pre-tRNA and the L15/16 domain of the enzyme affects the release step of the reaction (*18*). Beebe *et al*. (*19*) showed that the 3′-CCA sequence of a pre-tRNA also takes part in catalytic centre formation by interacting with the catalytic Mg^{2+} ion. Lazard and other researchers showed that the bases of the 5′-leader region adjacent to the cleavage site affect the cleavage efficiency of the substrate (*20–24*). These results demonstrate the importance of both the 5′-leader sequence and the 3′-NCCA tag sequence of a substrate in recognition by the enzyme. On the other hand, cross-linking studies showed the interaction of the surface of the enzyme with the T-arm (*25–27*), the D-arm (*28*) and the top half of the pre-tRNA (*29*). Many researchers have accepted that the interactions at the 5′ and 3′ termini are major determinants of substrate recognition and that interactions at other sites are minor. The cleavage site selection model by Kirsebom and Svard should be right, but there are still many exceptions that cannot be explained with their model. Something important, we suppose, has been disregarded in the understanding of substrate recognition by this enzyme.

The role of the protein subunit in substrate shape recognition is complicated and has therefore been seen as an enigma. The bacterial ribozyme comprises an RNA

*To whom correspondence may be addressed. Tel: +81-53-244-6920, Fax: +81-53-244-6929, E-mail: tanakat@eco.tut.ac.jp

subunit and a small protein subunit (*30*). Structural and cross-linking studies showed that the protein subunit sits on the surface of the RNA subunit to contact the 5′-leader region of a pre-tRNA (*31–34*); this protein accepts the 5′-leader region of the substrate, countervailing the surface charge between the enzyme and the substrate (*35–37*). As the above studies show, the protein subunit promotes the enzymatic activity of the ribozyme. However, when we compare the substrate shape specificities of the ribozyme and holoenzyme, the role of the protein subunit is hard to understand. The shape specificity of the ribozyme is always broadened in the presence of the protein subunit (*38–41*). Interestingly, the broadened shape specificity of the holoenzyme is altered to be narrower of the ribozyme-type in the presence of the 30S subunit of the ribosome (*42*). On the other hand, another cross-linking study showed that the protein subunit contacts the P12 domain of the RNA subunit on the opposite side of the substrate-binding site in the computer-modelled structure (*43*). These data suggest that the protein subunit of the RNase P takes part in substrate recognition through interaction with the flexible region of the ribozyme. To date, the flexible region of the ribozyme has been thought to be the specificity (S-) domain, which includes the P12 domain (*44*). But the substrate recognition mechanism remains unclear.

Therefore, we focused on the substrate shape specificity of this ribozyme. In a previous study, we prepared a series of bottom-half variant pre-tRNAs and showed that both the RNase P ribozyme and the holoenzyme demonstrate strict shape specificity towards these RNAs, but the holoenzyme cannot distinguish a pre-tRNA from a hairpin RNA mimicking the top half of a pre-tRNA (*45*). The results indicate that the bottom half takes part in substrate recognition by the ribozyme, suggesting the presence of a subsite for recognition of this part of a pre-tRNA. For further analysis, we prepared and examined other types of shape-variant pre-tRNAs in this study.

MATERIALS AND METHODS

Preparations of RNAs and Protein—The gene encoding every pre-tRNA variant was chemically synthesized and cloned into a commercial vector (pGEM-3Z, Promega) as described (*45*). The pre-tRNA variants were prepared *in vitro* and were labelled at the 5′-end with [γ-^{32}P]ATP and polynucleotide kinase for cleavage site analysis, or were internally labelled with [α-^{32}P]UTP for kinetic analyses as described (*45*). The *E. coli* RNase P ribozyme subunit was prepared *in vitro* from a pGEM-3Z-derived plasmid, and the protein subunit was prepared from *E. coli* BL21(DE3) cells harbouring a pET3a-derived plasmid that encodes the gene for the protein, as described (*38*). Holoenzyme was reconstituted from the ribozyme and protein subunits.

The secondary structure of each RNA was examined with ribonucleases V1 and S1 (Pierce) using 3′-end labelled RNA, as described (*46*).

Cleavage Site Analysis and Kinetic Analysis—We examined the cleavage site and the cleavage efficiency of these RNAs by using the ribozyme and holoenzyme. Reactions were done under standard conditions (1.4 nM pre-tRNA variant, 50 nM ribozyme + 50 nM protein subunit, 50 mM Tris–HCl, 5 or 10 mM $MgCl_2$ for ribozyme reactions and 2.5 mM for holoenzyme reactions, 100 mM NH_4Cl, 5% [w/v] polyethylene glycol-6000; 37°C, pH 7.6, 90 min, 30 μl) (*45*). The reactions were stopped by the addition of EDTA solution to a final concentration of 20 mM. The products were developed in 20% polyacrylamide by PAGE, and were quantitatively analyzed.

For the kinetic analyses, the enzymatic activities were measured at 37°C, pH 7.6 (50 mM Tris–HCl, 100 mM NH_4Cl, 5% [w/v] polyethylene glycol-6000). For ribozyme reactions, 30 μl of reaction mixture additionally contained 5 or 10 mM $MgCl_2$, 4–500 nM each substrate, and 2, 5 or 10 nM ribozyme. For holoenzyme reactions, 25 μl of reaction mixture additionally contained 2 mM $MgCl_2$, 4–500 nM each substrate, and 2, 10 or 40 nM reconstituted holoenzyme. Each RNA was preincubated for 2 min at 75°C, and then was refolded at 37°C. The reactions were stopped by the addition of EDTA solution to give a final concentration of 20 mM. After development in 20% polyacrylamide containing 8 M urea by PAGE, the radioactivities of the bands were analysed with a BAS-1800 phosphor imager (Fujifilm). The cleavage velocity of the substrate RNA was calculated from the initial cleavage rate of the substrate by multiple turnover kinetics. The kinetic parameters were determined from the standard Michaelis–Menten equation.

RESULTS AND DISCUSSION

Cleavage Site Analysis of Shape Variants of a Pre-tRNA—We prepared two series of shape variants for this study: T-stem length-variant RNAs and acceptor-stem length-variant RNAs (Fig. 1). Seven acceptor-stem length variant RNAs—A4, A5, A6, A7 (wild-type), A8, A9 and A10 (the number denotes the length of the acceptor-stem)—have a common sequence except in the 3′-end strand by engineering of a pre-tRNA^{Val} (Fig. 1B). Four T-stem length-variant RNAs—T4, T5 (wild-type), T6 and T7 (the number denotes the length of the T-stem)—have a common RNA sequence except in the length of the T-stem by insertion or removal of C–G or G–C base pairs (Fig. 1C). The secondary structure of these variant RNAs was examined with ribonucleases V1 and S1: *e.g.* the result of A5 variant was shown with that of wild-type pre-tRNA (Fig. 2). The secondary structure of each, at least of the top-half part, was the same cloverleaf shape as the wild-type pre-tRNA. The cleavage reactions of these variant RNAs were examined by both RNase P ribozyme and holoenzyme. The products were developed on 20% PAGE. The results of the ribozyme reactions at 5 mM Mg^{2+} are shown in Fig. 3A and B, and those of the ribozyme reactions at 10 mM Mg^{2+} and of the holoenzyme reactions at 2.5 mM Mg^{2+} are summarized in Fig. 3C.

Efficient cleavage of A7 (wild-type) and A8 RNAs occurred at the same cleavage site, between N^{-1} and N^{+1} (Fig. 3A). The cleavage of A9 was less efficient, and that of A4, A5 and A6 was faint. The cleft product of A10 was not detected. The cleavage efficiency of A4, A5, A6 and A10 was raised in the presence of a higher concentration

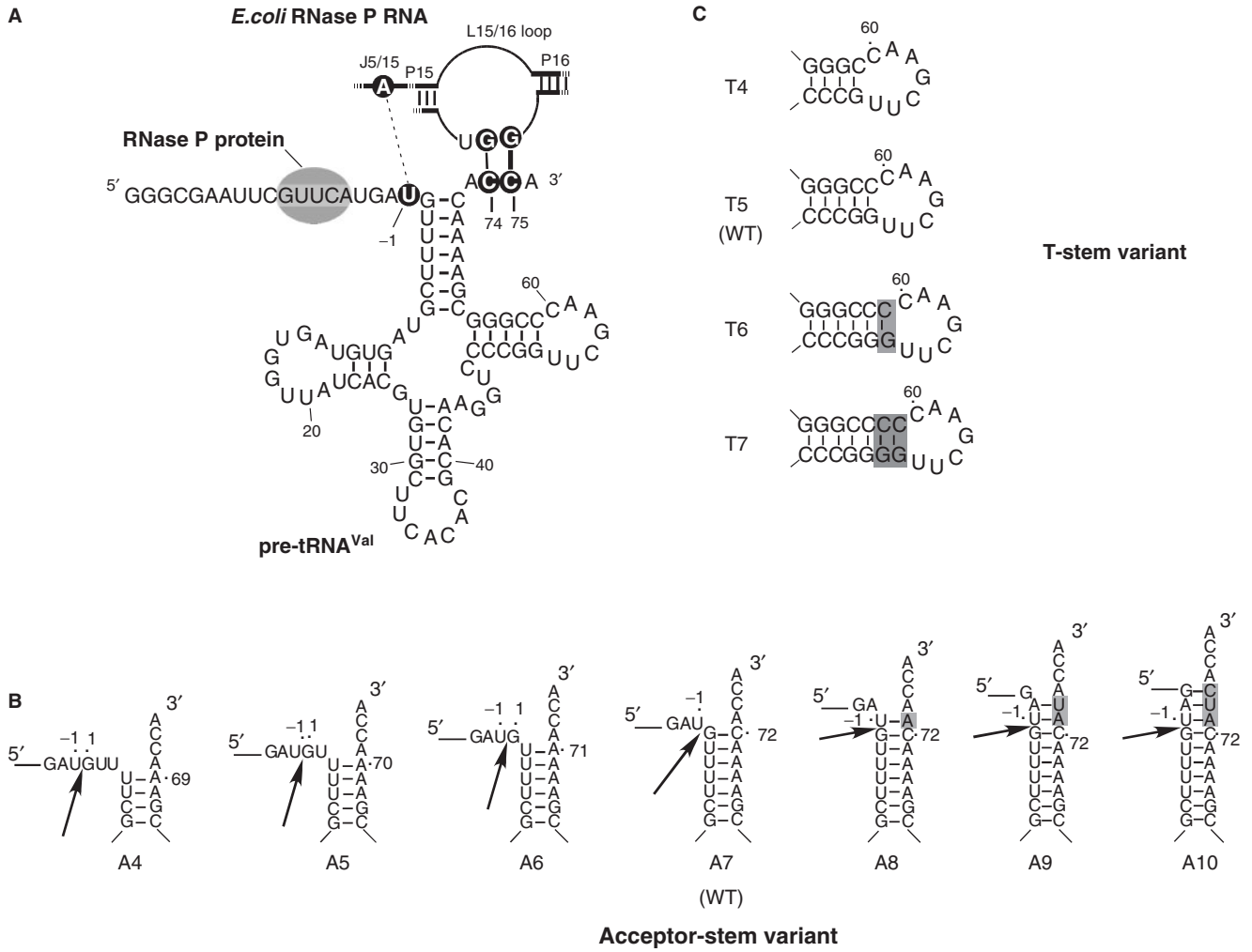

Fig. 1. **Summary of known RNase P RNA-pre-tRNA interactions and partial secondary structures of pre-tRNA variant RNAs used in this study.** (A) A pre-tRNA^{Val} is shown with the L15/16 loop of *E. coli* RNase P NA. Highlighted nucleotides mark the sites for Watson–Crick base pair bonding (*24*, *34*). The putative interaction site of the P protein to the 5′-leader region of a pre-tRNA is also shown (*32*). (B) Partial secondary structures of the accepter-stem variant RNAs. Arrows indicate the cleavage site by the ribozyme and the holoenzyme (see RESULTS). The variant RNA 'A7' corresponds to the wild-type pre-tRNA. The 'A4', 'A5' and 'A6' RNAs lack $A^{70}A^{71}C^{72}$, $A^{71}C^{72}$ and C^{72}, respectively. The 'A8', 'A9' and 'A10' RNAs have additional A, AU and AUC base(s) between C^{72} and A^{73}, respectively. (C) Partial secondary structures of the T-stem variant RNAs. The variant 'T5' corresponds to the wild-type pre-tRNA. The 'T4' RNA lacks the C^{61}–G^{53} base pair. The 'T6' and 'T7' RNAs have additional one and two C–G base pair(s), respectively.

of Mg^{2+} or in the presence of the protein subunit (Fig. 3C). The cleavage site of the substrate was not affected by the addition of higher amount of Mg^{2+} or the protein subunit. The results indicate that the ribozyme preferred the wild-type pre-tRNA (A7) at low Mg^{2+}. The substrate preference of the ribozyme at 10 mM Mg^{2+} and the preference of the holoenzyme at 2.5 mM Mg^{2+} were not clear, because A7, A8 and A9 were efficiently hydrolyzed. Both the ribozyme and the holoenzyme prefer longer acceptor-stem RNAs to shorter.

Efficient cleavage of T5 (wild-type) and T6 RNAs occurred at the same cleavage site, between N^{-1} and N^{+1} (Fig. 3B). The cleavage of T4 and T7 was detected at the same site but was faint. The efficiency of cleavage of T4 and T7 by the ribozyme at 10 mM Mg^{2+} and by the holoenzyme at 2.5 mM Mg^{2+} remained low (Fig. 3C). The cleavage site was not affected by the addition of higher amount of Mg^{2+} or the protein subunit. The results indicate that both the ribozyme and the holoenzyme prefer the wild-type pre-tRNA (T5) under the conditions examined, and that both prefer longer T-stem RNAs to shorter.

To confirm the cleavage site of RNAs, the detailed analysis was done. For example, the results of A5, A9, of which the cleavage site is of focus, and wild-type RNAs were shown in Fig. 4. We have confirmed the cleaved site of variant RNAs was same with the wild-type pre-tRNA, between N^{-1} and N^{+1}. The results also showed the presence of the protein component and the presence of high concentration of magnesium ions did not affect the cleavage site selection.

The above results indicate that both the holoenzyme and the ribozyme had strict substrate shape preference when a tRNA-like shape-variant RNA was presented.

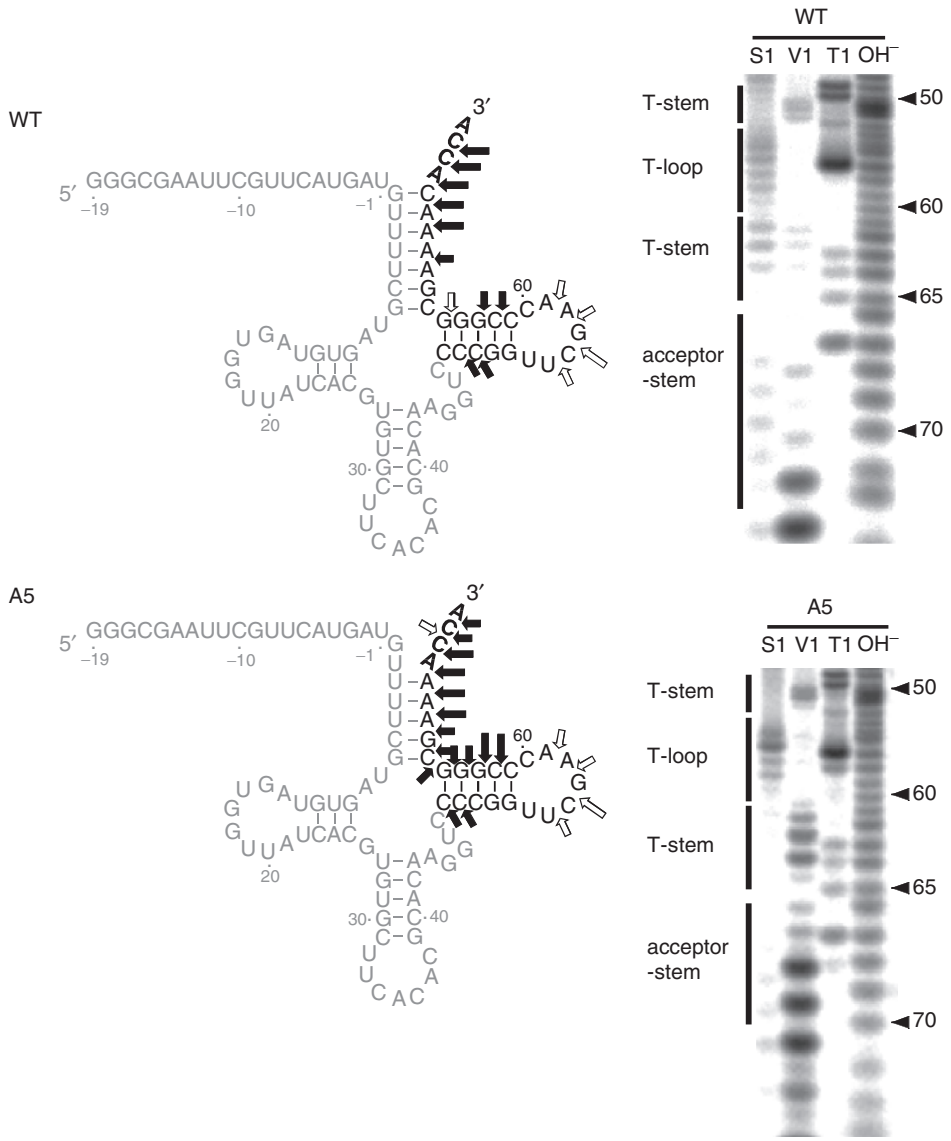

Fig. 2. **Secondary structure analysis on variant RNAs.** The results of wild-type pre-tRNA (*top*) and A5 variant RNA (*bottom*) were shown. The putative secondary structure of the RNA was shown in cloverleaf shape (*left*). The closed and open arrows represent the cleaved sites by RNase V1 and S1, respectively. The results of PAGE analysis were also shown (*right*). 'S1', 'V1' and 'T1' represent the products treated with RNase S1, V1 and T1, respectively. 'OH$^-$' represents the partially alkaline hydrolyzed products. Numbers on the right-hand of the photo represent the base position.

The holoenzyme distinguished a pre-tRNA from other tRNA-like RNAs, even though it cannot distinguish a pre-tRNA from a hairpin RNA. Interestingly, the results of the acceptor-stem variant indicated that the cleavage site selection of the substrate did not obey the rule demonstrated by Kirsebom and Svard: the cleavage site of every RNA was between N^{-1} and N^{+1}, being independent of the position of the 3′-CCA sequence of the substrate.

Subsites for Recognition of the T-Arm and the Bottom Half of a Pre-tRNA—Our results indicate that the cleavage site of the pre-tRNA is not always determined by the position of the 3′-CCA sequence of the substrate RNA. Both the T-arm and the bottom half of the pre-tRNA played an important role in the cleavage reaction and affected the cleavage efficiency (see Fig. 3 and ref. *45*). Efficient cleavage occurred only when these parts of the substrate were present in the correct positions. These facts mean that the RNase P ribozyme and the holoenzyme interact with the T-arm and the bottom half independently in the reaction, meaning there are two subsites in the substrate-binding site of the enzyme (Fig. 5A).

Our subsite model includes a major cleft, of about 12 base pairs' length, on the surface of the substrate-binding site, which is probably shown in the computer-modelled tertiary structure. The major cleft is large enough to accept the hairpin of the top half of a pre-tRNA, but not the whole T-arm and the bottom half. The T-arm site should be a pocket at the end of the major cleft.

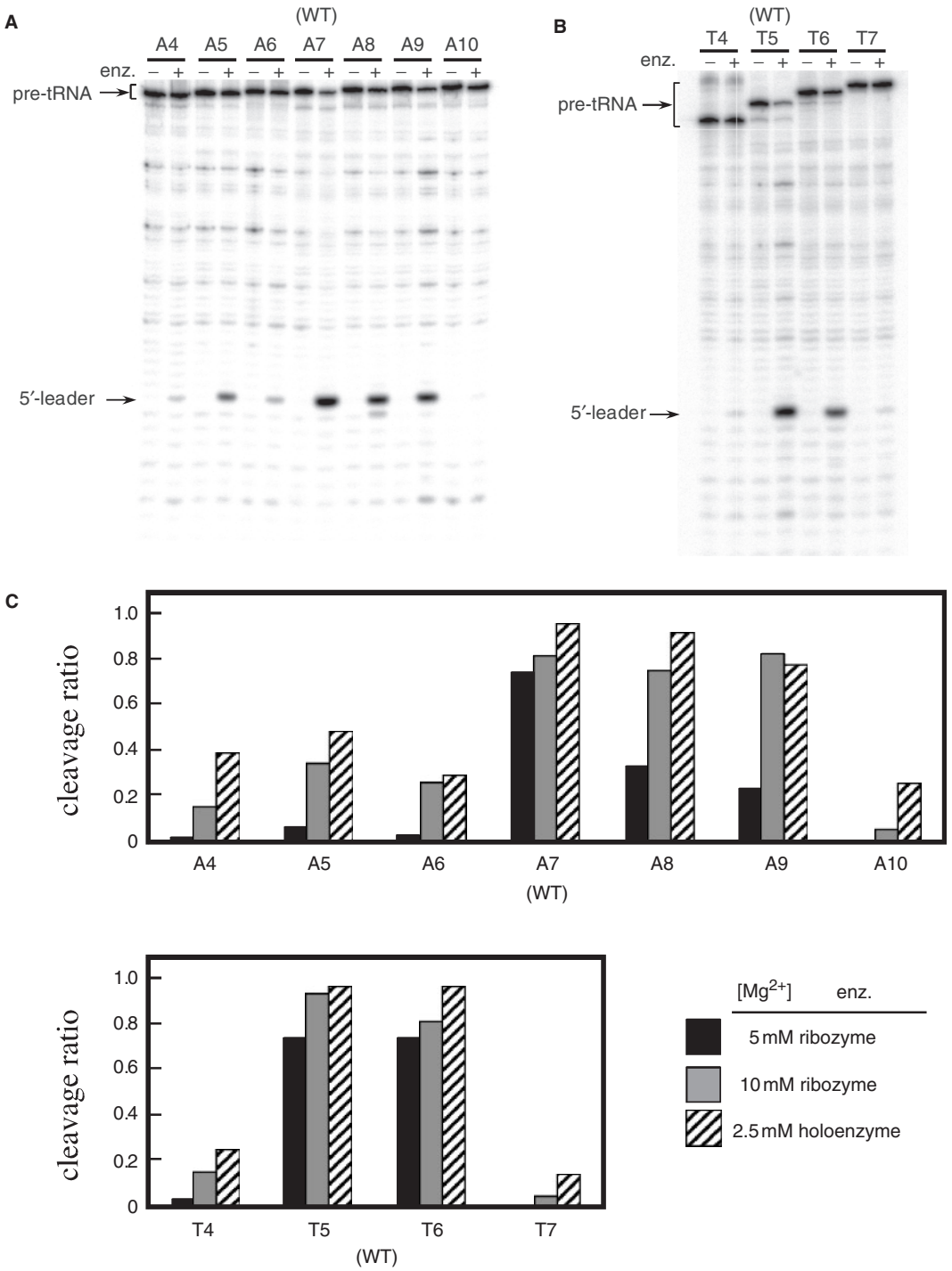

Fig. 3. **PAGE analysis for cleavage site and efficiency of shape variant RNAs of pre-tRNA by ribozyme.** (A) Results of accepter-stem length variant RNAs. (B) Results of T-stem length variant RNAs. '+' and '–' represent the reaction in the presence and absence of the ribozyme, respectively. Reactions were done under the standard ribozyme reaction conditions at the concentration of 5 mM magnesium ions. (C) Summary of apparent cleavage efficiency of the shape variant RNAs by the ribozyme at 5 and 10 mM magnesium ion concentrations and by the holoenzyme at 2.5 mM magnesium ion concentrations.

The bottom-half site should be a narrow cleft near the T-arm site (Fig. 5A, *left*). When a canonical L-shape pre-tRNA is bound to the substrate-binding site, the 5′ and 3′ termini of the pre-tRNA are trapped on the 5′-leader and the CCA sites, respectively, and both the T-arm and part of the bottom half (probably the D-arm) are bound to the T-arm and the bottom-half sites, respectively (Fig. 5A, *right*). The anticodon-arm of the substrate faces away from the substrate-binding site and does not take part in substrate specificity.

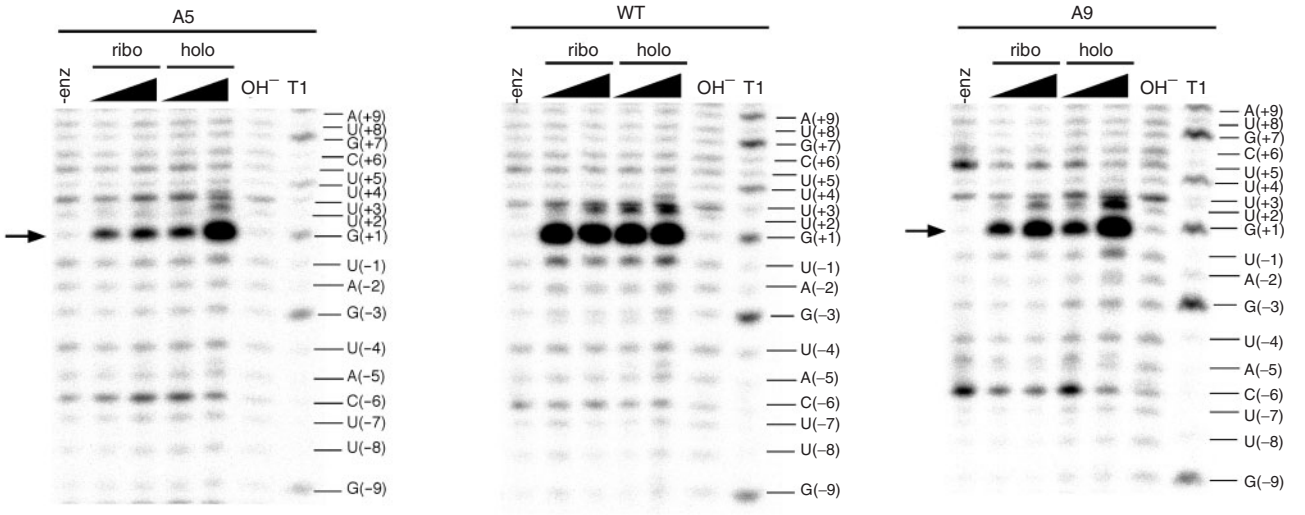

Fig. 4. **Detailed cleavage site analysis of RNAs.** The results of A5 (*left*), wild-type (*centre*) and A9 (*right*) RNAs were shown. 5′-end labelled RNA was used as a substrate. The results of Fig. 3C were used. The contrast of the photograph was tuned to visualize all products including spontaneously hydrolyzed products which are otherwise invisible. '-enz', 'OH$^-$' and 'T1' represent the product in the absence of ribozyme, the partially alkaline hydrolyzed ladder marker, and the ribonuclease T1-treated products, respectively. The base positions are shown on the right-hand side of the photo. The reactions were done by ribozyme at 5 or 10 mM magnesium ion concentrations, or by reconstituted holoenzyme at 2.5 or 5 mM magnesium ion concentrations. The arrow on the left-hand of the photo shows the position of the 5′-leader product.

The interactions between the T-arm and its cognate site and between the bottom half and its cognate site stabilize the reaction intermediate (probably the transition state; discussed later) or provide positive binding energy for the occurrence of the reaction.

Once the presence of these subsites is assumed, the cleavage site selection by the enzyme is easily explained (Fig. 5B). When a pre-tRNA in a canonical shape comes into the substrate-binding site, each of its four parts—the 3′-CCA, the 5′-leader sequence, the T-arm and the bottom half—is bound to the cognate subsite, and the interactions provide the positive binding energy for the enzymatic reaction. When a bottom-half variant RNA comes to the enzyme, the top half of the substrate is first trapped by three sites—the CCA site, the 5′-leader site, and the T-arm site—and the position of the bottom half is examined later. If the bottom half of the RNA is in the correct position, this part is accepted by the bottom-half site of the ribozyme and the reaction occurs. But if the bottom half is in the wrong position, the essential interactions at the bottom half are deficient, and the presence of this bulky part on the substrate-binding cleft perturbs or inhibits the enzyme reaction. The negative binding energy comes from the interactions of the bulky bottom half in the wrong position and the substrate-binding cleft of the enzyme is, we suppose, very high and cannot be compensated for by the presence of a high concentration of Mg^{2+} or the protein subunit.

The recognition of the T-stem variants is similar to that of the bottom-half variants. When the T-stem variant RNA comes to the enzyme, the RNA is first trapped by three sites—the CCA site, the 5′-leader site and the bottom-half site—and the shape of the T-arm is examined later. When the T-stem of the RNA is shorter or longer, the interactions at the T-arm site are deficient, and the presence of this bulky T-arm on the substrate-binding cleft perturbs or inhibits the enzyme reaction. The interactions at both the bottom half and the T-arm are essential for the occurrence of the ribozyme reaction at a low concentration of Mg^{2+}. The interactions at these subsites determine the site of substrate cleavage by the enzyme. When an acceptor-stem variant comes to the enzyme, the RNA is trapped by three subsites—the 5′-leader site, the bottom-half site and the T-arm site—and the position of the CCA sequence is examined later. If the position of the 3′-CCA of a substrate is acceptable, the substrate is cleft by the enzyme at the usual position between N^{-1} and N^{+1}, neglecting the position of the 3′-CCA sequence.

Our model can explain the substrate shape specificity observed. For the occurrence of the ribozyme reaction at low Mg^{2+} concentration, the interactions at both the bottom half and the T-arm are essential. When a hairpin RNA mimicking the top half of a pre-tRNA comes to the substrate-binding site of the ribozyme, this RNA is able to fit into the large cleft because it has no bulky extra part with it (*39*). The interactions at the CCA site, the 5′-leader site, and the T-arm site occur, but they are not enough for the occurrence of the enzyme reaction because the essential interaction at the bottom half is deficient. The presence of a high concentration of Mg^{2+} or the protein subunit can compensate for the interactions at the bottom half (the role of these cofactors in substrate recognition is discussed later). Our results appear to contradict those of Kirsebom and Svard, who held that the position of the 3′-CCA determines the site of cleavage by the enzyme. There are many exceptions to the model of the determination of the cleavage site by the 3′-CCA sequence. For example, *E. coli* and *B. subtilis* ribozymes cleave a hairpin RNA derived from fly pre-$tRNA_i^{Met}$ at

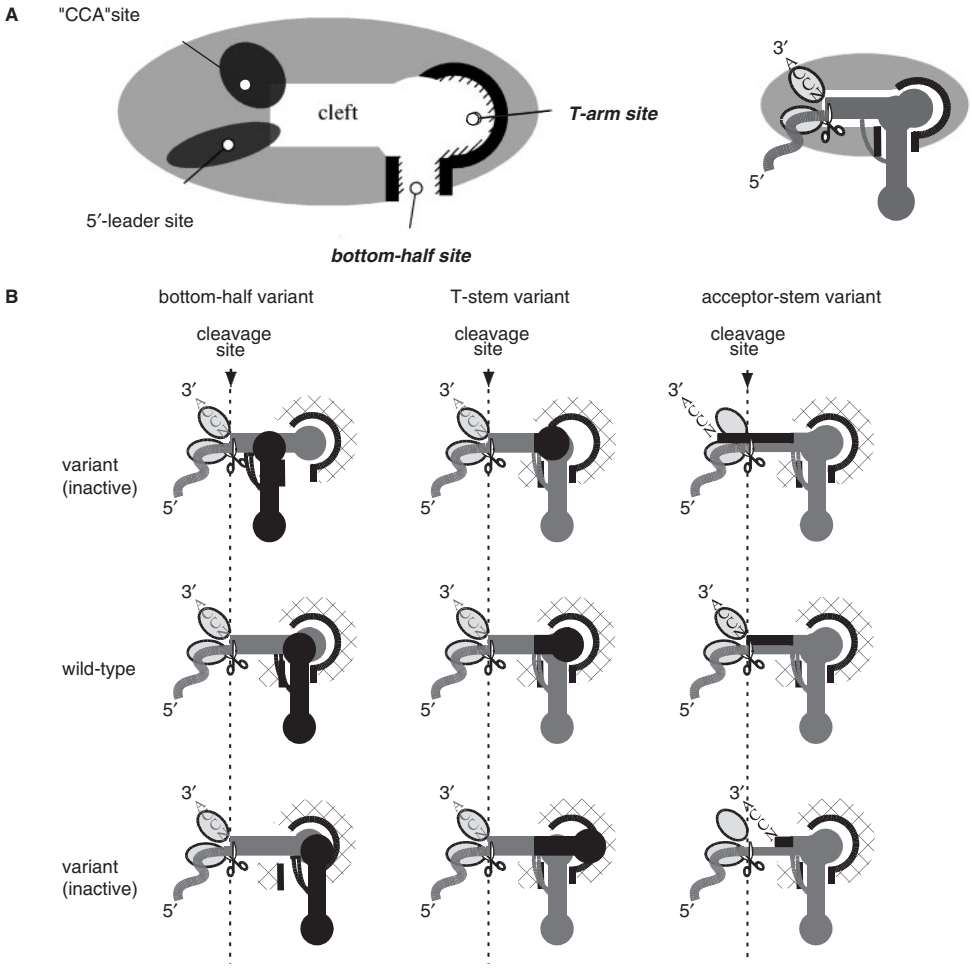

Fig. 5. **Schematic representation of subsites of RNase P RNA.** (A) Subsites are shown with (*right*) and without (*left*) a pre-tRNA substrate. The whole ribozyme subunit is shown as an oval (*grey*), and the walls of the subsites for the bottom-half part and the T-arm are shown as solid line and curves with hatched lines. The CCA site and the 5′-leader site represent the accepter of the 3′-NCCA terminus and the 5′-leader region of a substrate, respectively, as shown in Fig. 1. The T-arm and the bottom-half sites locate on the opposite side of the CCA and 5′-leader sites of the major substrate binding cleft. The bottom-half site should be a narrow cleft, which accepts the part of the bottom half (probably around the D-arm) of a pre-tRNA. (B) Schematic representation for cleavage site selection. Three series of shape variant RNAs are summarized with the subsites (*open circle* or *solid curve and line*): the bottom-half part-shifting variant RNAs (*left*), the T-stem length variant RNAs (*centre*), and the accepter-stem length variant RNAs (*right*). The results of bottom-half part-shifting variant RNAs are from the previous report (*45*); other results were done in this study. The cleavage site by the enzyme was shown with the common constant region (*grey*) and the engineered region (*black*) of the RNA. In case of the bottom-half variant RNAs, the 5′ and 3′ termini and the T-arm of the RNA (*grey*) take part in cleavage site selection, and the position of the bottom-half (*black*) determines the cleavage efficiency (*left*). If the position of the bottom half is acceptable by the cognate subsite, the cleavage reaction occurs but at low efficiency. In case of the T-stem variant RNAs, the 5′ and 3′ termini and the bottom half of the RNA (*grey*) take part in cleavage site selection, and the position of the T-arm (*black*) determines the cleavage efficiency (*centre*). If the engineered T-arm is acceptable by the cognate subsite, the cleavage reaction occurs but at low efficiency. And, in case of the accepter-stem variant RNAs, the 5′ terminus, the T-arm and the bottom half (*grey*) take part in the cleavage site selection, and the position of the 3′-CCA (*black*) determines the cleavage efficiency (*right*). If the position of the 3′-CCA is able to form the active centre, the cleavage reaction occurs but at low efficiency.

N^{-1}–N^{+1}, N^{+1}–N^{+2} and N^{+2}–N^{+3}, one derived from human pre-$tRNA^{Tyr}$ at N^{-2}–N^{-1} and N^{-1}–N^{+1}, and one derived from human pre-$tRNA_3^{Lys}$ at N^{-2}–N^{-1}, N^{+1}–N^{+2} and N^{+3}–N^{+4} (the numbering indicates the position relative to the 3′-NCCA in the hairpin form) (*46*, *47*). We have also shown that the cleavage site of a hairpin RNA from the human pre-$tRNA^{Tyr}$ shifts from N^{-2}–N^{-1} to N^{-1}–N^{+1} as the concentration of Mg^{2+} increases (*47*). These results indicate that the cleavage site selection does not always depend on the position of the 3′-CCA sequence of the pre-tRNA: it is affected also by the concentration of Mg^{2+} and by the shape of the substrate. Here, we claim that the interactions at both the bottom half and the T-arm outweigh the interaction at the CCA site in determining the enzyme reaction. When an RNA with a bottom half and a T-arm of the correct shapes comes into the substrate-binding cleft, the interactions at both subsites settle the substrate to a certain position and determine

Table 1. **Kinetic parameters for the hydrolysis of acceptor-stem length variant RNAs by *E. coli* RNase P ribozyme and holoenzyme.**

	k_{cat} (ratio) $\times 10^{-3}$ min^{-1}	K_M (ratio) nM	k_{cat}/K_M (ratio) M^{-1}min^{-1}
Ribozyme			
[Mg]: 5 mM			
A5	ND	ND	ND
A6	ND	ND	ND
A7 (WT)	91 ± 3.9 (1.0)	325 ± 31 (1.0)	2.8×10^5 (1.0)
A8	24 ± 1.0 (0.3)	353 ± 35 (1.1)	6.7×10^4 (0.2)
A9	23 ± 0.8 (0.3)	316 ± 26 (1.0)	7.3×10^4 (0.3)
[Mg]: 10 mM			
A5	83 ± 4.4 (0.4)	165 ± 19 (1.1)	5.1×10^5 (0.3)
A6	18 ± 0.9 (0.08)	133 ± 15 (0.9)	1.4×10^5 (0.1)
A7 (WT)	223 ± 11 (1.0)	146 ± 16 (1.0)	1.5×10^6 (1.0)
A8	52 ± 2.7 (0.2)	226 ± 24 (1.6)	2.3×10^5 (0.1)
A9	45 ± 1.0 (0.2)	135 ± 8.4 (0.9)	3.3×10^5 (0.2)
Holoenzyme			
A5	25 ± 0.1 (0.1)	87 ± 11 (0.8)	2.8×10^5 (0.2)
A6	26 ± 0.9 (0.1)	52 ± 5.9 (0.5)	4.9×10^5 (0.3)
A7 (WT)	185 ± 9.1 (1.0)	112 ± 14 (1.0)	1.6×10^6 (1.0)
A8	49 ± 3.4 (0.3)	54 ± 12 (0.6)	9.1×10^5 (0.6)
A9	31 ± 2.0 (0.2)	125 ± 24 (1.1)	2.5×10^5 (0.2)

'ND' represents 'not determined', because of low cleavage activity. The values in parenthesis are the values relative to those of WT (defined as 1.0). 'A7' corresponds the wild-type pre-tRNA.

Table 2. **Kinetic parameters for the hydrolysis of T-stem length variant RNAs by *E. coli* RNase P ribozyme and holoenzyme.**

	k_{cat} (ratio) $\times 10^{-3}$ min^{-1}	K_M (ratio) nM	k_{cat}/K_M (ratio) M^{-1}min^{-1}
Ribozyme			
[Mg]: 5 mM			
T4	ND	ND	ND
T5 (WT)	91.4 ± 3.9 (1.0)	325 ± 30 (1.0)	2.8×10^5 (1.0)
T6	25.8 ± 0.4 (0.3)	394 ± 9.4 (0.9)	8.8×10^4 (0.3)
[Mg]: 10 mM			
T4	25 ± 2.0 (0.1)	250 ± 2.0 (1.7)	9.9×10^4 (0.07)
T5 (WT)	223 ± 11 (1.0)	146 ± 16 (1.0)	1.5×10^6 (1.0)
T6	95 ± 7.5 (0.7)	109 ± 21 (0.6)	8.8×10^5 (0.6)
Holoenzyme			
T4	7.6 ± 0.0 (0.04)	43 ± 3.3 (0.4)	1.8×10^5 (0.1)
T5 (WT)	185 ± 9.1 (1.0)	112 ± 14 (1.0)	1.6×10^6 (1.0)
T6	81 ± 4.4 (0.4)	92 ± 13 (0.8)	8.8×10^5 (0.5)

'ND' represents 'not determined', because of low cleavage activity. The values in parenthesis are the values relative to those of WT (defined as 1.0). 'T5' corresponds the wild-type pre-tRNA.

the cleavage site first, and the catalytic centre cleaves the bond later if the 3′-CCA is successfully positioned to form the catalytic core.

As seen above, our subsite model is consistent with all experimental results but should be modified to explain the role the protein subunit and additional higher amount of Mg^{2+} ions. To understand in detail how the enzyme recognizes the substrate, we performed kinetic analyses of the shape-variant RNAs.

Kinetic Analyses of Shape Variant RNAs—We determined the kinetic parameters of the shape-variant RNAs by standard multiple-turnover Michaelis–Menten kinetics to analyse how and when the enzyme recognizes the substrate shape. We prepared internally labelled RNAs, and the reaction products were developed on 20% PAGE and the kinetic parameters were calculated from the intensity of cleaved products. The results are summarized in Tables 1 and 2. We did ribozyme reactions at 5 or 10 mM Mg^{2+} and holoenzyme reactions at 2 mM Mg^{2+}. The addition of the protein subunit and of Mg^{2+} to the ribozyme tended to raise the cleavage efficiency by raising the affinity between the enzyme and the substrate or by raising the hydrolysis rate of the substrate. The substrate shape preference appears consistent with the results shown in Fig. 2: the ribozyme and the holoenzyme prefer the wild-type pre-tRNA, and prefer longer acceptor-stems and T-stems to shorter.

Comparison of the kinetic parameters indicated that the difference in substrate shape affected mainly the magnitude of the k_{cat} values, not that of the K_M values. This tendency was also observed in the results of the bottom-half variant RNAs, as reported previously (*45*). The transition state theory says that the magnitude of the K_M value correlates to the binding energy of the enzyme and the substrate in forming the Michaelis complex, and the magnitude of the k_{cat} value corresponds to the activation energy of the substrate–enzyme complex from the non-transition state to the transition state (please note that we took 'Michaelis-complex' as substrate-enzyme complex in 'non-transition state' in this article) (*48*). We summarized the results of kinetic analyses as a simple model of substrate recognition below.

Substrate Recognition Model—The substrate recognition model is shown in Fig. 6. According to the transition state theory as explained above, the difference in shape, the length of the top-half and the position of the bottom half, had little or no effect on the Michaelis complex (ES) formation, and the substrate shape affected mainly the activation of the substrate–enzyme complex from the Michaelis complex (ES) to the transition state ($ES^{\ddagger}$). This means that on the acceptance of the substrate RNA onto the enzyme, in the Michaelis complex formation step the length of the top-half and the position of the bottom half are neglected first, and the bottom half and T-arm subsites do not take part in substrate acceptance. The remaining two subsites—the CCA site and the 5′-leader site—we suppose play an important role in this step. The energy of binding between the partial structure of the substrate and the cognate subsite of the enzyme helps to stabilize the following transition-state conformation. In this step, the bottom half and the T-arm take part in substrate shape recognition. After cleavage of the 5′-leader sequence, the interactions at the 5′-leader site become deficient, and the enzyme–product complex (EP_1) returns to the non-transition-state conformation. In this step, the interactions at the CCA site temporally remain (*18*). The product (P_1) is then released from the enzyme.

The above recognition model is consistent with the data of Kirsebom and Svard as described above, because we agree that the 3′-NCCA sequence of a pre-tRNA plays a dominant role in substrate accepting- and

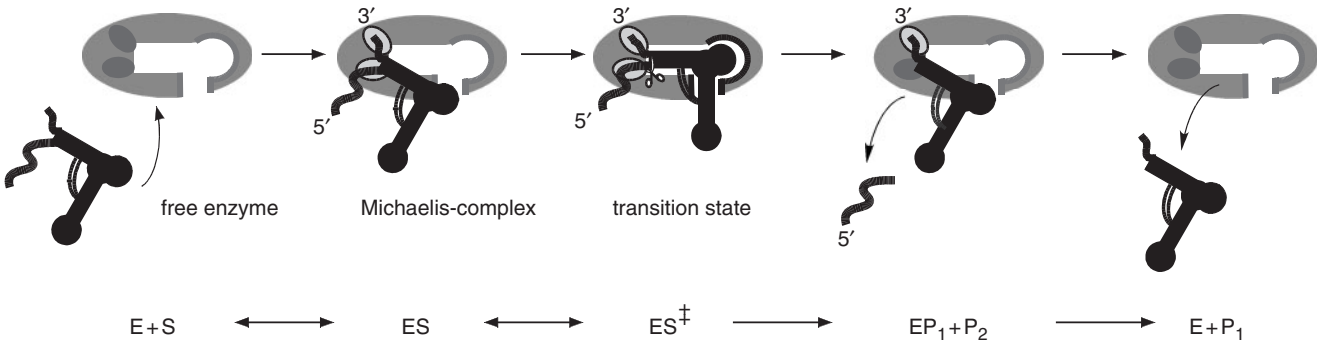

Fig. 6. **Substrate recognition model.** The grey oval represents the whole structure of the ribozyme (E). Scissors present the catalytic centre. Subsite is colored in grey for 'inactive' or blue for 'active'. A pre-tRNA is trapped on the CCA site and 5'-leader site first to form the Michaelis-complex (ES). On this step, the shape of a substrate RNA is not recognized by the enzyme. After that, the T-arm site and the bottom-half site cooperatively examine the shape of the substrate to achieve the transition state ($ES^{‡}$) conformation. After the cleavage of the 5′-leader sequence, the enzyme-product complex (EP_1) turns to the nontransition state conformation, and the cleaved product (P_1) is released from the enzyme.

releasing-steps. Our model is also consistent with the claim by Harris *et al*. (*34*) that the enzyme and substrate first interact at the 5′ and 3′ termini.

Of course, there is a possibility of movement of the flexible domain of the ribozyme in the transition state formation step; however, the compilation of evidence is not enough. In this model, we do not mention about the structure or conformation of the enzyme in the transition state, nor the relationship between the mobile domain of the ribozyme and the transition state stabilization: we have a hypothetical extended model based on this substrate recognition model, which can explain the role of the protein subunit and the effect of the Mg^{2+} bound at high concentrations, and which will be reported it in future.

We have shown the presence of two subsites—the bottom half and the T-arm—in the substrate-binding site. The substrate shape is recognized by the enzyme mainly in the transition state of the reactions. From these facts, we propose a substrate recognition model. We are convinced that our work has helped to explain the ribozyme RNase P.

ACKNOWLEDGEMENTS

We are thankful to Ms Etsuko Sakai and Mr Hiromichi Suzuki for radioisotope operations. This work was supported by a Grant-in-Aid for Scientific Research on Priority Areas from the Ministry of Educations, Culture, Sports, Science, and Technology of Japan.

CONFLICT OF INTEREST

None declared.

REFRENCES

1. Altman, S. and Kirsebom, L.A. (1999) *The RNA world* (Gesteland, R.F., Cech, T.R., and Atkins, J.F. eds), pp. 351–419. Cold Spring Harbor Laboratory Press, Cold Spring Harbor, NY
2. Westhof, E. and Altman, S. (1994) Three-dimensional working model of M1 RNA, the catalytic RNA subunit of ribonucelase P from *Escherichia coli*. *Proc. Natl Acad. Sci. USA* **91**, 5133–5137
3. Massire, C., Jaeger, L., and Westhof, E. (1998) Derivation of the three-dimensional architecture of bacterial ribonucelase P RNAs from comparative sequence analysis. *J. Mol. Biol.* **279**, 773–793
4. Tsai, H.Y., Masquida, B., Biswas, R., Westhof, E., and Gopalan, V. (2003) Molecular modeling of the three dimensional structure of the bacterial RNase P holoenzyme. *J. Mol. Biol.* **325**, 661–675
5. Haas, E.S., Morse, D.P., Brown, J.W., Schmidt, F.J., and Pace, N.R. (1991) Long-range structure in ribonuclease P RNA. *Science* **254**, 853–856
6. Schmitz, Z. and Tinoco, I. (1999) NMR solution studies on the P4 element of bacterial RNase P RNA. *FASEB J.* **13**, A1323–A1323
7. Krasilnikov, A. S., Yang, X., Pan, T., and Modragon, A. (2003) Crystal structure of the specificity domain of ribonuclease P. *Nature* **421**, 760–764
8. Warnecke, J.P., Fürste, J.P., Hardt, W.D., Erdmann, V.A., and Hartmann, R.K. (1996) Ribonuclease P RNA is converted to a Cd^{2+}-ribozyme by a single Rp-phophorothioate modification in the precursor tRNA at the RNase P cleavage site. *Proc. Natl Acad. Sci. USA* **93**, 8924–8928
9. Christian, E.L., Kaye, N.M., and Harris, M.E. (2000) Helix 4 is a divalent metal ion binding site in the conserved core of the ribonuclease P ribozyme. *RNA* **6**, 511–519
10. Zuleeg, T., Hartmann, R.K., Kreutzer, R., and Limmer, S. (2001) NMR spectroscopic evidence for Mn^{2+} (Mg^{2+}) binding to a precursor-tRNA microhelix near the potential RNase P cleavage site. *J. Mol. Biol.* **305**, 181–189
11. Kaye, N.M., Christian, E.L., and Harris, M.E. (2002) NAIM and site-specific functional group modification analysis of RNase P RNA: magnesium dependent structure within the conserved P1-P4 multihelix junction contributes to catalysis. *Biochemistry* **41**, 4533–4545
12. Tanaka, T., Ando, T., Haga, S., and Kikuchi, Y. (2004) Examining the bases of J3/4 domain of *Escherichia coli* ribonuclease P. *Biosci. Biotechnol. Biochem.* **68**, 1388–1392
13. Tanaka, T., Kanda, N., and Kikuchi, Y. (2004) The P3 domain of *E. coli* ribonuclease P RNA is able to be truncated and replaceable. *FEBS Lett.* **577**, 101–104
14. Haga, S., Tanaka, T., and Kikuchi, Y. (2004) Mutational analyses on the length of J3/4 domain of *Escherichia coli* ribonuclease P ribozyme. *Biosci. Biotechnol. Biochem.* **68**, 2630–2632
15. Kaye, N.M., Zahler, M.H., Christian, E.L., and Harris, M.E. (2002) Conservation of helical structure contributes to functional metal ion interactions in the catalytic domain of ribonuclease P RNA. *J. Mol. Biol.* **324**, 429–442

16. Kirsebom, L.A. and Svard, S.G. (1994) Base pairing between *Escherichia coli* RNase P RNA and its substrate. *EMBO J.* **13**, 4870–1876
17. Oh, B.K., Frank, D.N., and Pace, N.R. (1998) Participation of the 3′-CCA of tRNA in the binding of catalytic Mg^{2+} ions by ribonuclease P. *Biochemistry* **37**, 7277–7283
18. Tallsjo, A., Kufel, J., and Kirsebom, L.A. (1996) Interaction between *Escherichia coli* RNase P RNA and its discriminator base results in slow product release. *RNA* **2**, 299–307
19. Beebe, J.A., Kurz, J.C., and Fierke, C.A. (1996) Magnesium ions are required by *Bacillus subtilis* ribonuclease P RNA for both binding and cleaving precursor $tRNA^{Asp}$. *Biochemistry* **35**, 10493–10505
20. Lazard, M. and Meinnel, T. (1998) Role of base G^{-2} of pre-$tRNA^{fMet}$ in cleavage site selection by *Escherichia coli* RNase P *in vitro*. *Biochemistry* **37**, 6041–6049
21. Christian, E.L. and Harris, M.E. (1999) The track of the pre-tRNA 5′ leader in the ribonuclease P ribozyme-substrate complex. *Biochemistry* **38**, 12629–12638
22. Pascal, A. and Vioque, A. (1999) Substrate binding and catalysis by ribonuclease P from cyanobacteria and *Escherichia coli* are affected differently by the 3' terminal CCA in tRNA precursors. *Proc. Natl Acad. Sci. USA* **96**, 6672–6677
23. Loria, A. and Pan, T. (1999) The cleavage step of a ribonuclease P catalysis is determined by ribozyme-substrate interactions both distal and proximal to the cleavage site. *Biochemistry* **38**, 8612–8620
24. Brannvall, M., Pettersson, B.M.F., and Kirsebom, L.A. (2003) Importance of the +73/294 interaction in *Escherichia coli* RNase P RNA substrate complexes for cleavage and metal ion coordination. *J. Mol. Biol.* **325**, 697–709
25. Baer, M.F., Reilly, R.M., McCorkle, G.M., Hai, T.Y., Altman, S., and RajBhandary, U.L. (1988) The recognition by RNase P of precursor tRNAs. *J. Biol. Chem.* **263**, 2344–2351
26. Harris, M.E., Kazantsev, A.V., Chen, J.L., and Pace, N.R. (1997) Analysis of the tertiary structure of the ribonuclease P ribozyme-substrate complex by site-specific photoaffinity crosslinking. *RNA* **3**, 561–576
27. Loria, A. and Pan, T. (1997) Recognition of the T stem-loop of a pre-tRNA substrate by the ribozyme from *Bacillus subtilis* ribonuclease P. *Biochemistry* **36**, 6317–6325
28. Hardt, W.D., Schlegl, J., Erdmann, V.A., and Hartmann, R.K. (1993) Role of the D arm and the anticodon arm in tRNA recognition by eubacterial and eukaryotic RNase P enzymes. *Biochemistry* **32**, 130446–13053
29. Loria, A., Niranjanakumari, S., Fierke, C.A., and Pan, T. (1998) Recognition of a pre-tRNA substrate by the *Bacillus subtilis* RNase P holoenzyme. *Biochemistry* **37**, 15466–15473
30. Pannucci, J.A., Haas, E.S., Hall, T.A., Harris, J.K., and Brown, J.W. (1999) RNase P RNAs from some archaea are catalytically active. *Proc. Natl. Acad. Sci. USA* **96**, 7803–7808
31. Stams, T., Niranjanakumari, S., Fierke, C.A., and Christianson, D.W. (1998) Ribonuclease P protein structure: Evolutionary origins in the translational apparatus. *Science* **280**, 752–755
32. Niranjanakumari, S., Stams, T., Crary, S.M., Christianson, D.W., and Fierke, C.A. (1998) Protein component of the ribozyme ribonuclease P alters substrate recognition by directly contacting precursor tRNA. *Proc. Natl Acad. Sci. USA* **95**, 15212–15217
33. Gopalan, V., Hühne, H., Biswas, R., Li, H., Bruwig, G.W., and Altman, S. (1999) Mapping RNA-protein interactions in ribonuclease P from *Escherichia coli* using electron paramagnetic resonance spectroscopy. *Biochemistry* **38**, 1705–1714
34. Sun, L., Campbell, F.E., Zahler, N.H., and Harris, M.E. (2006) Evidence that substrate-specific effects of C5 protein lead to uniformity in binding and catalysis by RNase P. *EMBO J.* **25**, 3998–4007
35. Reich, C., Olsen, G.J., Pace, B., and Pace, N.R. (1988) Role of the protein moiety of ribonuclease P, a ribonucleoprotein enzyme. *Science* **239**, 178–181
36. Rox, C., Feltens, R., Pfeiffer, T., and Hardmann, R.K. (2002) Potent contact sites between the protein and RNA subunit in the *Bacillus subtilis* RNase P holoenzyme. *J. Mol. Biol.* **315**, 551–560
37. Kurz, J.C., Niranjanakumari, S., and Fierke, C.A. (1998) Protein component of *Bacillus subtilis* RNase P specifically enhances the affinity for precursor-$tRNA^{Asp}$. *Biochemistry* **37**, 2393–2400
38. Ando, T., Tanaka, T., and Kikuchi, Y. (2003) The protein component of bacterial RNase P flickers the metal ion response of the substrate shape preference of the ribozyme. *Biosci. Biotechnol. Biochem.* **67**, 2294–2296
39. Ando, T., Tanaka, T., and Kikuchi, Y. (2003) Substrate shape specificity of *Escherichia coli* RNase P ribozyme is dependent on the concentration of magnesium ion. *J. Biochem.* **133**, 445–451
40. Park, B.H., Lee, J.H., Kim, M., and Lee, Y. (2000) Effects of C5 protein on *Escherichia coli* RNase P catalysis with a precursor $tRNA^{Phe}$ bearing a single mismatch in the acceptor stem. *Biochem. Biophys. Res. Commun.* **268**, 136–140
41. Tanaka, T., Baba, H., Hori, Y., and Kikuchi, Y. (2001) Guide DNA technique reveals that the protein component of bacterial ribonuclease P is a modifier for substrate recognition. *FEBS Lett.* **491**, 94–98
42. Barrera, A. and Pan, T. (2004) Interaction of the *Bacillus subtilis* RNase P with th 30S ribosomal subunit. *RNA* **10**, 482–492
43. Sharkady, S.M. and Nolan, J.M. (2001) Bacterial ribonuclease P holoenzyme crosslinking analysis reveals protein interaction sites on the RNA subunit. *Nucleic Acid Res.* **29**, 3848–3856
44. Qin, H., Sosnick, T.R., and Pan, T. (2001) Modular construction of a tertiary RNA structure: the specificity domain of the *Bacillus subtilis* RNase P RNA. *Biochemistry* **40**, 11202–11210
45. Tanaka, T., Nagai, Y., and Kikuchi, Y. (2005) Substrate shape preference of *Escherichia coli* ribonuclease P ribozyme and holo enzyme using bottom-half part-shifting variants of pre-tRNA. *Biosci. Biotechnol. Biochem.* **69**, 1992–1994
46. Hori, Y., Baba, H., Ueda, R., Tanaka, T., and Kikuchi, Y. (2000) *In vitro* hyperprocessing of *Drosophila* tRNAs by the catalytic RNA of RNase P: the cloverleaf structure of tRNA is not always stable? *Eur. J. Biochem.* **267**, 4781–4788
47. Tanaka, T., Kondo, Y., Hori, Y., and Kikuchi, Y. (2002) Another cut for lysine tRNA: application of the hyperprocessing reaction reveals another stabilization strategy in metazaon lysine tRNAs. *J. Biochem.* **131**, 839–847
48. Fersht, A. (1985) *Enzyme Structure and Mechanism*. Freeman, Oxford, UK